Supplementary Information for

Enhancing Tumor Accumulation and Cell Uptake of Layered Double Hydroxide Nanoparticles by Coating/Detaching pH-Triggered Charge-Convertible Polymer

Tiefeng Xu[†,$,#], *Jianping Liu*[‡,#], *Luyao Sun*[‡], *Run Zhang*[‡], *Zhi Ping Xu*[‡,*], *Qing Sun*[†,*]

[†] Shandong Qianfoshan Hospital, Cheeloo College of Medicine, Shandong University, Jinan City, Shandong Province 250014, China.

[$] The First Affiliated Hospital and The Oncological Institute of Hainan Medical University, Haikou City, Hainan Free Trade Port 570102, China.

[‡] Australian Institute for Bioengineering and Nanotechnology (AIBN), The University of Queensland, St Lucia, QLD 4072, Australia

[#] These authors contribute equally to this work.

* Corresponding authors.

Email: qingsw99@163.com (Qing Sun)

Email: gordonxu@uq.edu.au (Z. P. Xu)

Contents:

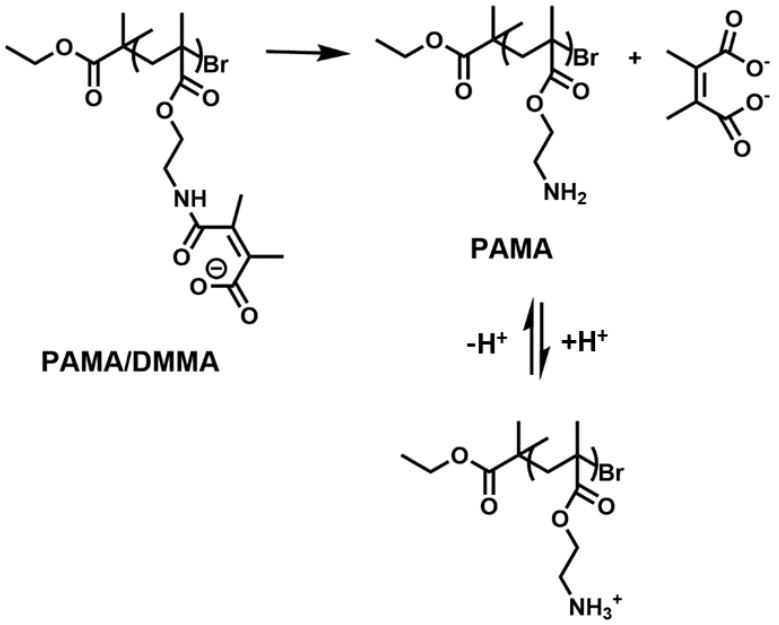

Scheme S1. Mechanism of charge conversion of PAMA/DMMA at pH 6.8.

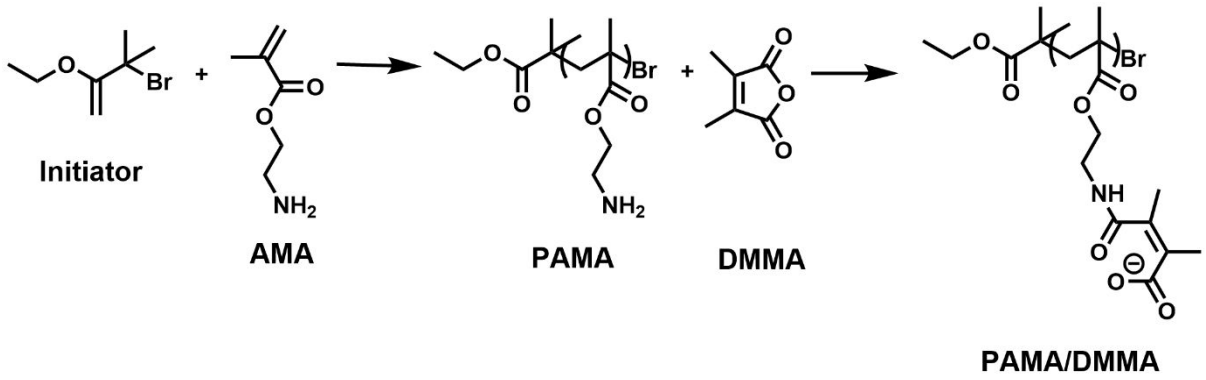

Scheme S2. Synthesis route of PAMA/DMMA.

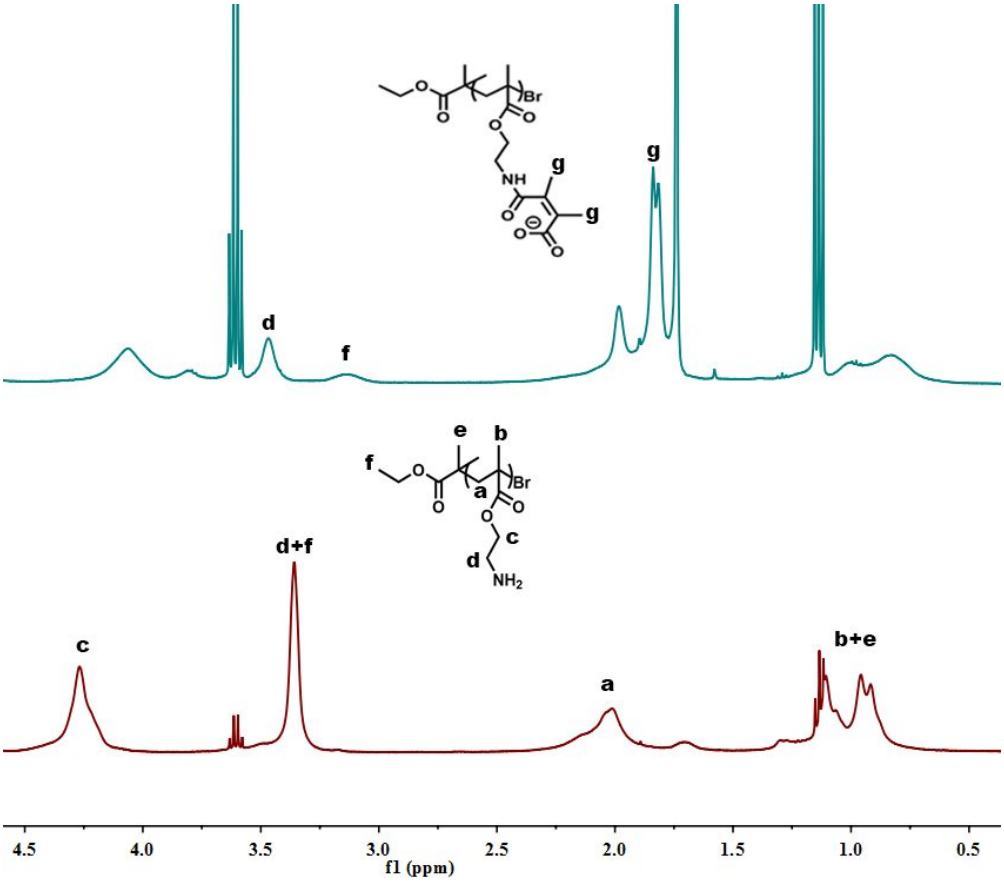

Figure S1. ^{1}H NMR spectra of PAMA and PAMA/DMMA.

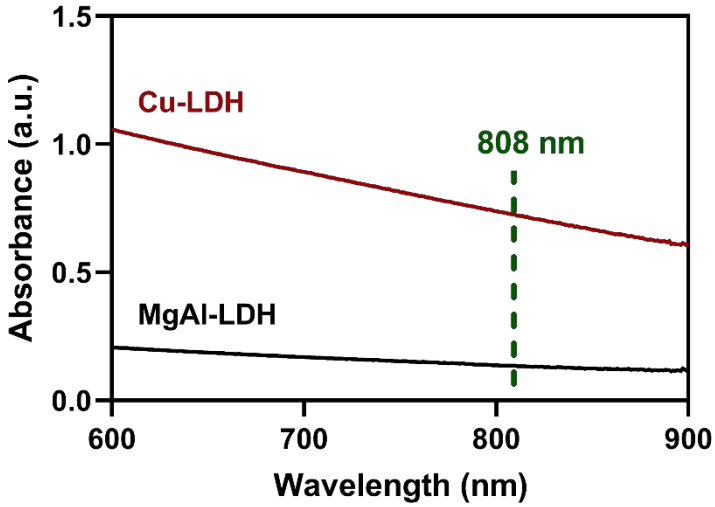

Figure S2. UV-Vis spectrum of Cu-LDH at [Cu] = 125 µg/mL.

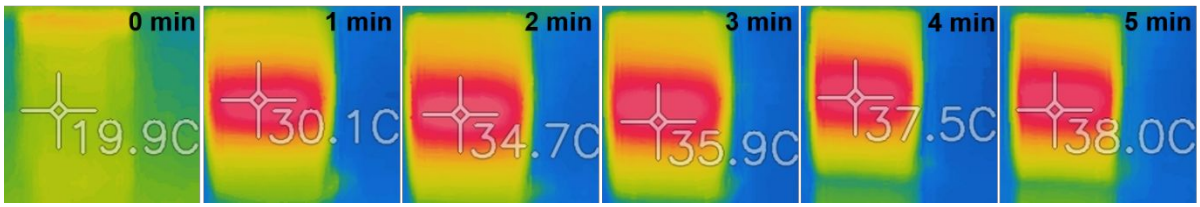

Figure S3. Infrared thermal images of deionized water and aqueous Cu-LDH nanoparticles with different copper concentrations ([Cu]: 125 μg/mL) under 808 nm laser irradiation with a power density of 1.0 W/cm^2 for 5 min.

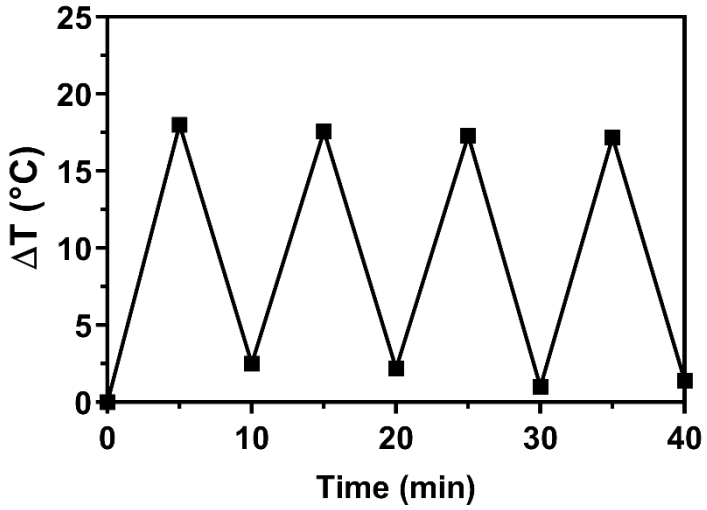

Figure S4. Photostability tests of Cu-LDH suspension for five cycles at [Cu] = 125 μg/mL under 808 nm laser irradiation with a power density of 1.0 W/cm^2 for 5 min.

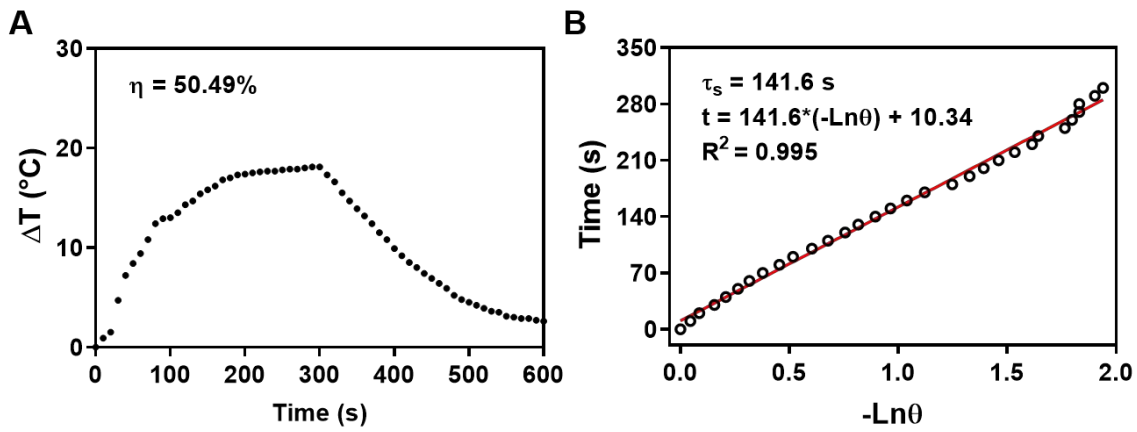

Figure S5. (A) Temperature profiles of Cu-LDH irradiated with 808 nm laser for 300 s, followed by a natural cooling for 300 s (laser was turned off). (B) The determination of system time constant (τ_s) calculated by the linear regression of the 300 s-cooling profile of Cu-LDH.

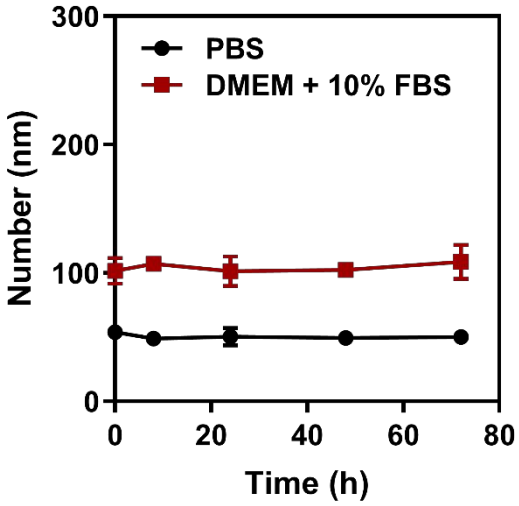

Figure S6. Colloidal stability of Cu-LDH@PAMA/DMMA in PBS and DMEM with 10 % FBS.

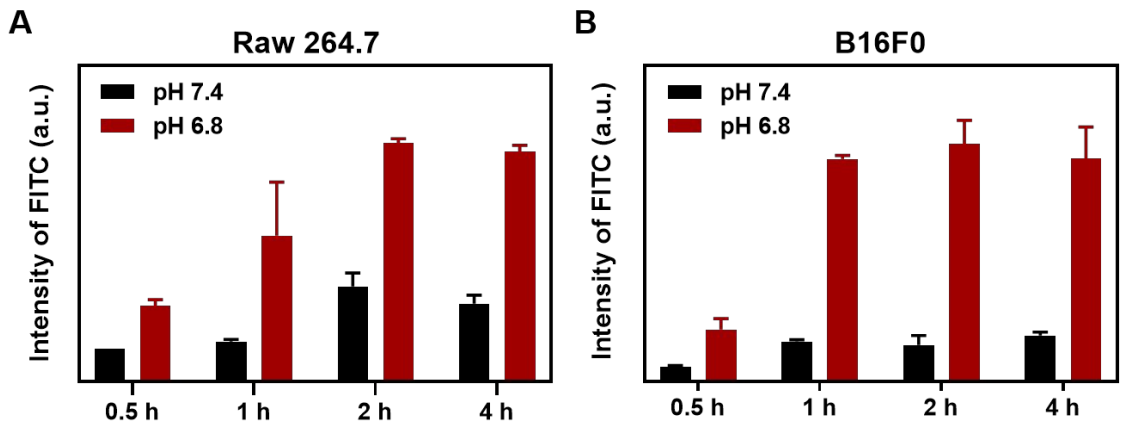

Figure S7. Time-dependent cellular uptake of Cu-LDH@PAMA/DMMA in Raw 264.7 cells (A) and B16F0 cells (B).

Table S1. GPC data of PAMA and PAMA/DMMA.

Polymers	M_n (Da)	M_w (Da)	PDI	DP
PAMA*n*	4685	5209	1.112	28
PAMA/DMMA*n*	6988	7388	1.057	18

Table S2. Size and Zeta potential of Cu-LDH@PAMA/DMMA at different mass ratios of PAMA/DMMA to LDH.

PAMA/DMMA : Cu-LDH	Cu-LDH@PAMA/DMMA		
	Number (nm)	PDI	Zeta (mV)
Cu-LDH	39.4	0.115	+33.7
5:1	52.2	0.112	-26.6
4:1	53.7	0.112	-25.2
3:1	50.9	0.126	-25.6
2:1	90.9	0.127	-21.9
1:1	120.6	0.141	-11.5
0.5:1	152.1	0.373	-8.3
0.2:1	283.4	0.412	-6.9

Table S3. Coating content calculated based on the carbon amounts of nanoparticles and TGA analysis.

Method	Elements	Cu-LDH[#]	Cu-LDH@PAMA/DMMA
ICP	Cu	15	-
	Mg	15.5	-
	Al	8	-
CHN	C	0.8	32.6
	H	3.9	5.1
	N	0	4.1
	(Est. Coating)	-	66.2*
TGA	Weight Loss	42.1	83.4
	(Est. Coating)	-	71.3[$]

[#] The approximate chemical formula was $Cu_{0.8}Mg_{2.2}Al(OH)_8Cl_{0.6}(CO_3^{2-})_{0.2}\cdot 2H_2O$.

* The weight % was estimated based on C weight % as the polymer contains 48.4% C in their chemical formula.

[$] The weight % was estimated from the weight loss in TGA by the following equation:

coating wt% = measured weight loss % of coated Cu-LDH – measured weight loss % of Cu-LDH × weight percent of Cu-LDH,

where weight percent of Cu-LDH is 100% – coating wt%. Here polymer or BSA was supposed to all decompose at 800 ^oC in arial TGA and the weight loss was read at 800 ^oC.

Table S4. Comparison of various Cu-based nanoparticles for magnetic resonance imaging (MRI).

Nanomaterials	**r1 (mM^{-1} s^{-1})**	**Magnetic field**	**Ref**
CuS	0.26 0.12	3.0 T 7.0 T	[1] [2]
$CuCl_2$	0.21	9.4 T	[3]
Cu oleate	4.02	3.0 T	[4]
Cu_3P	0.59	3.0 T	[5]
CuO	0.38	9.4 T	[6]
Cu-LDH	0.98 (pH 7.4) 2.83 (pH 6.0)	16.0 T	This work

References

(1) Chu, Z.; Wang, Z.; Chen, L.; Wang, X.; Huang, C.; Cui, M.; Yang, D.-P.; Jia, N. Combining magnetic resonance imaging with photothermal therapy of CuS@BSA nanoparticles for cancer theranostics. *ACS Appl. Nano Mater.* **2018,** *1*, 2332-2340.

(2) Xia, C.; Xie, D.; Xiong, L.; Zhang, Q.; Wang, Y.; Wang, Z.; Wang, Y.; Li, B.; Zhang, C. Nitroxide radical-modified CuS nanoparticles for CT/MRI imaging-guided NIR-II laser responsive photothermal cancer therapy. *RSC Adv.* **2018,** *8*, 27382-27389.

(3) Ge, R.; Lin, M.; Li, X.; Liu, S.; Wang, W.; Li, S.; Zhang, X.; Liu, Y.; Liu, L.; Shi, F.; Sun, H.; Zhang, H.; Yang, B. Cu^{2+}-loaded polydopamine nanoparticles for magnetic resonance imaging-guided pH- and near-infrared-light-stimulated thermochemotherapy. *ACS Appl. Mater. Interfaces* **2017,** *9*, 19706-19716.

(4) Pan, D.; Caruthers, S. D.; Senpan, A.; Yalaz, C.; Stacy, A. J.; Hu, G.; Marsh, J. N.; Gaffney, P. J.; Wickline, S. A.; Lanza, G. M. Synthesis of NanoQ, a copper-based contrast agent for high-resolution

magnetic resonance imaging characterization of human thrombus. *J. Am. Chem. Soc.* **2011,** *133*, 9168-9171.

(5) Liu, Y.; Wu, J.; Jin, Y.; Zhen, W.; Wang, Y.; Liu, J.; Jin, L.; Zhang, S.; Zhao, Y.; Song, S.; Yang, Y.; Zhang, H. Copper(I) phosphide nanocrystals for in situ self-generation magnetic resonance imaging-guided photothermal-enhanced chemodynamic synergetic therapy resisting deep-seated tumor. *Adv. Funct. Mater.* **2019,** *29*, 1904678.

(6) Perlman, O.; Weitz, I. S.; Azhari, H. Copper oxide nanoparticles as contrast agents for MRI and ultrasound dual-modality imaging. *Phys. Med. Biol.* **2015,** *60*, 5767.